

Design Optimization of Wireless Access Virtualization Based on Cost & QoS Trade-Off Utility Maximization

M. Moshir Rahman, *Student Member, IEEE*, Charles Despins, *Senior Member, IEEE*, and Sofiène Affes, *Senior Member, IEEE*

Abstract—Wireless access virtualization is an emerging avenue for research for future 5G networks. For its ability to augment network sharing and its subsequent impact on reducing network setup and operational costs, network virtualization is greatly sought after by telecommunications operators all over the world. This paper classifies virtual wireless access into three possible PHY-MAC models that differ in terms of the degree of segregation of baseband signal processing and radio access units. One of the models uses special purpose hardware while another leverages software defined networking (SDN) and cloud computing technologies for implementing virtual wireless access using general purpose hardware. The proposed models differ in terms of their associated network operational cost as well as in terms of the level of QoS they can provide. A new multi-criteria utility function is hence proposed in order to assess the tradeoffs between network cost & QoS of these models from a PHY-MAC layer perspective. The new utility function provides guidelines for a network designer to choose the optimal virtualization model that best fits an operator's budget constraint as well as the QoS requirement of the intended service. Analytical results show that a novel hybrid model that properly combines both special purpose and SDN & cloud computing technologies maximizes the newly introduced utility function by attaining the best balance between overall network cost and QoS. This occurs in most expected practical cases where precisely, one of the two does not relatively outweigh the other and viceversa.

Index Terms—Radio access networks, platform virtualization, cost benefit analysis, quality of service, PHY, MAC, SDN, cloud computing.

I. INTRODUCTION

TRADITIONAL cellular networks are designed to serve the peak network traffic demand. This often results

Manuscript received December 31, 2014; revised August 7, 2015 and January 20, 2016; accepted May 27, 2016. Date of publication June 14, 2016; date of current version September 8, 2016. This work was supported by an NSERC/Huawei Canada/TELUS CRD Grant on 5G-WAVES (WAV Enabling Schemes), the DG and CREATE PERSWADE (www.create-perswade.ca) Programs of NSERC, and a Discovery Accelerator Supplement Award from NSERC. The associate editor coordinating the review of this paper and approving it for publication was W. Wang.

M. M. Rahman is with the École de Technologie Supérieure, University of Quebec, Montreal, QC H3C 1K3, Canada (e-mail: mohamad-moshir.rahman.1@ens.etsmtl.ca).

C. Despins was with Prompt Inc., Montréal, QC H3B 3A7, Canada. He is now with École de Technologie Supérieure, University of Quebec, Montreal, QC H3C 1K3, Canada (e-mail: charles.despins@etsmtl.ca).

S. Affes is with the Institut National de la Recherche Scientifique, Centre Énergie, Matériaux et Télécommunications, University of Quebec, Montreal, QC H5A 1K6, Canada (e-mail: affes@emt.inrs.ca).

Color versions of one or more of the figures in this paper are available online at <http://ieeexplore.ieee.org>.

Digital Object Identifier 10.1109/TWC.2016.2580505

in over-provisioning of network resources [1], which is very expensive in terms of network deployment as well as operational costs. Network operators can not benefit from on demand resource provisioning which would allow them to scale-up or scale-down network resources according to traffic demand at any given instant of time. Moreover, the use of complex control plane protocols and vendor locked-in devices are not amenable to provision new cellular services that might require the implementation of novel protocols or signal processing schemes. Future 5G networks will demand a more flexible and elastic network architecture that will facilitate provisioning novel services at a lower network cost, which is not possible with current network architectures. To resolve these issues, it is imperative to re-architect current network structures in new ways that make most efficient use of available resources, use less expensive general-purpose hardware rather than expensive special-purpose hardware in order to reduce overall network cost and provide flexibility to incorporate new network technologies using programmable and elastic network infrastructure [2]. Virtualizing wireless access solves to a great extent the aforementioned problems.

In a virtual access topology, *independent and isolated* virtual networks are built on one or more physical network substrates in which the virtual networks are transparent to each other in terms of presence. The virtual networks are able to use customized network protocols, signal processing and network management functionalities that best suits the intended services. Wireless network virtualization has been approached from different perspectives: spectrum virtualization [3], [4], as well as virtualization for different wireless technologies (i.e., WLAN, WiMAX, LTE) [5]–[10]. Major telecommunication vendors and operators are teaming up for research in network function virtualization (NFV) [11]. The FP7-iJOIN project [12] is investigating the use of cloud computing for a radio access network as a service (RANaaS) paradigm, where RAN functionalities are distributed among decentralized and centralized network entities. The model focuses on handling interference in a dense network environment consisting of a large number of small (femto) cells. For front-haul, it uses either wireless or optical transmission links. Software defined networking (SDN) is being seen as a crucial driver to virtualize wireless access [2], [13], [14] and core [15], [16] networks due to its ability to introduce network flexibility by separating the control and data planes. Cloud computing is also being

investigated as a significant enabler towards a shared and elastic virtual wireless network [17]–[19].

Each of the aforementioned works tries to solve a particular problem pertaining to virtualization but a unified solution to wireless access network virtualization that incorporates virtualization of radio resources, computing & storage resources and the underlying network fabric is absent in the open literature. Different radio access technologies (RATs) use different physical, MAC and network layer processing techniques. Hence, a virtualization solution targeted to one particular RAT (e.g., WiFi) might not be applicable to another (e.g., 3G, long term evolution (LTE), etc.). In a complete virtualized platform, all network resources are virtualized. As such, it is not sufficient to virtualize processing and storage resources; the underlying network fabric must also be virtualized in order to create isolated virtual networks (VNs) on a shared infrastructure. Also provisions should be made for shared and isolated use of radio spectrum while maintaining service level agreements (SLA) between the infrastructure providers and the virtual network operators (VNOs). Hence, a unified solution to wireless network virtualization is necessary in order to facilitate shared and efficient resource utilization among incumbent VNOs, thus enabling them to implement a customized network using a common subset of network resources. Also the economic impact of various wireless virtualization models has not been analyzed in the available open literature according to the best knowledge of the authors of this paper.

In this paper, we classify wireless access virtualization frameworks in three different categories that vary in terms of their underlying physical infrastructures. We also analyze their respective network cost and achievable QoS trade-offs from PHY and MAC layer perspectives. This analysis provides guidance in selecting the best possible virtualization model for a certain implementation scenario. This paper claims the following contributions:

- The classification of virtual wireless access networks into three models (considering *greenfield* deployment scenarios).
- a) A special-purpose hardware-based wireless access virtualization model, referred to as Locally Virtualized Network (LVN), where a hypervisor is used to slice super base stations (SBSs) to create multiple virtual base stations (VBSs).
- b) A data center based wireless access virtualization model, referred to as Clustered/Remote Virtualized Network (CVN/RVN), where SDN and cloud computing technologies are used to virtualize the underlying networking fabric and computation & storage resources. In this model, fiber-distributed remote radio heads (RRHs) are used to provide radio access to users.
- c) A third model, referred to as hybrid virtualized network (HVN), where we properly combine both of the aforementioned models to offer the potential to balance network cost and QoS with greater flexibility than the previous two models (LVN and CVN/RVN).
- A new multi-criteria utility function that accounts for network cost & QoS trade-offs to enable the design

and optimization of wireless access virtualization architectures that best comply with the investment and service-level requirements of network operators (and/or service providers).

We present a LTE HetNet model as a benchmark to compare the current network deployment approach with the proposed virtualization frameworks. The remainder of this paper is structured as follows. In Section II, we briefly present the dimensioning, the cost analysis, and the time division duplex (TDD) configuration of a typical 4G LTE HetNet as a benchmark architecture without virtualization. In Sections III and IV, respectively, we analyze the virtualized architectures, the dimensioning, and both the capital expenditure (CAPEX) and operational expenditure (OPEX) calculations for the LVN and the CVN/RVN frameworks. Next, we subdue the HVN framework that we advocate in Section V to the same analysis exercise. The new network utility function is introduced and defined in Section VI, while analysis results are presented and discussed in Section VII. Conclusions are drawn out in Section VIII.

II. TRADITIONAL HETEROGENEOUS NETWORK (HETNET)

We consider here as a benchmark, an architecture without virtualization base on a multi-tier LTE HetNet consisting of macro, micro, and pico cells. It is pertinent to distinguish our network modeling with the models in [20] and [21]. The system model in [20] considers multiple radio interfaces per node that are capable of working on multiple channels. The paper focuses on the fact that, using multiple channels through multiple interfaces will enable higher bandwidth use, which will eventually result in higher system capacity. Though the authors consider heterogeneous channels and heterogeneous traffic, they do not consider a multi-tier heterogeneous network. The system model considered in [21] consists of a two-tier network having a macro-cell tier and a femto-cell tier and both are modelled following Poisson point process (PPP). Whereas in our paper, we consider a three-tier network model consisting of macro, micro and pico base stations, that are distributed across the coverage area following a deterministic distribution model. Moreover, we do not consider femto BSs (FBSs) in our analysis because FBSs are user owned devices that are deployed randomly according to the preference of users, which is beyond the control of cellular network operators.

A. HetNet Dimensioning

The HetNet model considered in our analysis consists of distributed smaller cells (micro, pico, and femto) with an overlay of large macro cells. While the macro cells provides network coverage, smaller cells are normally deployed to meet capacity demands in a certain area. To estimate the BS requirements, the total number of BSs needed to cover a certain area can be expressed as

$$N_{BS} = f(A, R_{BS}, R_{UE}, N_{UE}) \quad (1)$$

where N_{BS} is the total number of BSs, A is the coverage area, R_{BS} is the data rate capacity per BS, R_{UE} is the average data rate capacity demand per user equipment (UE) and N_{UE} is the average number of active UEs. A network can be modeled to

be either coverage or capacity limited. Hence a straightforward way to model the required number of BSs is [22]:

$$N_{BS} = \max\left(\frac{A}{\pi \times d_{BS}^2}, \frac{N_{UE} \times R_{UE}}{R_{BS}}\right) \quad (2)$$

where d_{BS} is the coverage radius of a BS. It should be noted that, in [22], only single-tier architectures are considered. The authors compared operational costs when the network consisted of any BS type (macro/micro/pico BSs). On the other hand, in this paper, we consider a three-tier heterogeneous network model that consists of macro, micro and pico BSs. We dimension the macro cells in coverage-limited cases in order to provide ubiquitous network coverage, whereas smaller cells (micro and pico) are deployed in capacity-limited cases, to satisfy user data rate demands.

B. HetNet Cost Analysis

The total cost per tier is the aggregate of capital expenditures (CAPEX), i.e., the initial set up cost of the network and operational expenditures (OPEX), i.e., the operational cost of the network per year for a specific tier. Hence the network cost for a tier i can be expressed as

$$C_i = N_{BS_i} \times (C_{cap_i} + C_{op_i}) \quad (3)$$

where C_i is the total cost for tier i , N_{BS_i} is the number of BSs in tier i , C_{cap_i} and C_{op_i} are the corresponding CAPEX and OPEX, respectively. Further, the CAPEX can be expressed as

$$C_{cap_i} = C_{eq_i} + C_{sb_i} \quad (4)$$

where C_{eq_i} and C_{sb_i} are the equipment and site-buildout costs, respectively. And the OPEX can be decomposed as

$$C_{op_i} = C_{sl_i} + C_{om_i} + C_{bh_i} \quad (5)$$

where C_{sl_i} , C_{om_i} , and C_{bh_i} are the site-lease cost, the operation and maintenance cost and the back-haul cost, respectively. The total cost for a K -tier HetNet is

$$C_T = \sum_{i=1}^K C_i. \quad (6)$$

We adopt the *cumulated discounted cash flow (DCF)* method [23] to calculate the total cost per tier i in present time. DCF analysis is a very commonly used valuation method to estimate the attractiveness of an investment opportunity, namely in terms of net present value (NPV). In this form of financial analysis, all the future cash flows are estimated and discounted to give their respective values in *present time*. DCF is based on the concept of time value of money, with variations in time due to inflation, capital gains, etc. Hence, in financial analysis, all future cash flows are estimated and discounted to give their present value.

In DCF analysis, to compute the NPV of an economic opportunity, all the future cash flow and a discount rate are given as input, and the output gives the NPV.

Mathematically, the discounted cost of an investment, c , at a discount rate of $d\%$, can be expressed as [23]

$$C = \frac{c}{(1+d)}. \quad (7)$$

In case, there are multiple cash-flows at future time periods, all future cash flows should be discounted and added together to get the NPV. For example, the NPV of a cash flow in P years can be calculated as [23]

$$C = \sum_{p=0}^{P-1} \frac{c_p}{(1+d)^p} \quad (8)$$

where c_p is the cash flow at year p and d is the discount rate. In our analysis, one BS is exploited for Y years, hence, for a discount rate d , the net NPV for the BS is

$$c = \sum_{y=0}^{Y-1} \frac{c_y^i}{(1+d)^y} \quad (9)$$

where c_y^i is the cost of a BS at tier i for the year y . Here, the CAPEX, i.e., the radio equipment, site buildout and site installation costs are accounted for the first year ($y = 0$). The annual OPEX (i.e., the site lease, O & M and backhaul costs) is assumed to be constant. The OPEX values are discounted for from $y = 1$ to $Y - 1$ years to calculate the net cost value in present time. Hence, c provides the net estimate (both investment and running costs) for the entire life-cycle of the BS in present values.

Adopting a similar approach, the total cost for the K -tier network that is exploited for Y years can be calculated as

$$\begin{aligned} C_{DT} &= \sum_{y=0}^{Y-1} \frac{C_{Ty}}{(1+d)^y} \\ &= \sum_{y=0}^{Y-1} \frac{\sum_{i=1}^K C_{iy}}{(1+d)^y} \\ &= \left(\sum_{i=1}^K C_{cap_i} + \sum_{y=1}^{Y-1} \frac{\sum_{k=1}^K C_{op_{ky}}}{(1+d)^y} \right) \times N_{BS_i} \quad (10) \end{aligned}$$

where in our analysis, the discount rate, d is assumed to be 10% and the BSs in the network are assumed to be used for $Y = 5$ years. The cost values used are given in (Table I [24]). Cost values used in the analysis are approximate, yet very representative. Since the goal of this article is to show the relative trend qualitatively rather than reporting exact cost values quantitatively, these representative values serve the purpose without impinging on the quality or nature of the obtained results and conclusions even if a more realistic setup were to be adopted instead. To keep our analysis tractable, it should be noted that we have assumed the discount rate d to be constant for the duration of the calculation time period, i.e., Y years. However, in practice, the discount rate may vary according to various factors, such as, the inflation rate, the financial risk involved in the opportunity, and the higher value of other opportunities.

TABLE I
 TRADITIONAL NETWORK BS PARAMETER

Parameter	MBS	MiBS	PBS
Cell range	700 m	175 m	70 m
Capacity (R_{BS})	300 Mbps	100 Mbps	100 Mbps
Radio equipment cost [\$k]	50	20	5
Site build-out [\$k]	70	-	-
Site installation [\$k]	30	15	3
O&M [\$k/year]	3	1	1
Site lease [\$k/year]	10	3	1
Backhaul transmission [\$k/year]	5	5	5

 TABLE II
 SPECIAL SUBFRAME CONFIGURATION FOR NORMAL CP

Special subframe configuration	CP in OFDM symbols		
	DwPTS	GP	UpPTS
0	3	8	1
1	8	3	1
2	9	2	1
3	10	1	1
4	3	7	2
5	8	2	2
6	9	1	2

Again, we would like to emphasize that the network cost calculated in [22] is targeted for a single-tier *homogeneous* network; in contrast, the cost model in Eq.(10) represents a *heterogeneous* network that consists of three different types of BSs deployed either in coverage-limited (macro BSs) or capacity-limited (micro and pico BSs) cases.

Femto BSs (FBSs) are customer-peripheral devices installed in a random manner. For this reason, we do not consider them in our modeling.

C. LTE-TDD Configuration

LTE operates in two different modes: Time Division Duplex (TDD) and Frequency Division Duplex (FDD). In our analysis, we have considered the TDD mode of operation due to its wide acceptance among mobile operators around the world [25], [26]. One other key motivation is that TDD, in contrast to FDD, could operate in full-duplex mode.

However, using TDD requires tight coordination and synchronization among network equipment in the same coverage area. For this reason, in TDD, the evolved nodes B (eNBs) operating in the same coverage area need to be synchronized with each other within the frame granularity. The switching electronics in the eNB and UE need time to toggle between the Tx/Rx modes. To facilitate this operation, a guard period (GP) is allocated in a special subframe to compensate for the switching time and the propagation delay. The special subframe mainly takes care of the DL-UL synchronization. This frame is structured in three parts: the Downlink Pilot Time Slot (DwPTS), the GP and the Uplink Pilot Time Slot (UpPTS). Table-II [27] shows the subframe configuration for LTE-TDD using a normal cyclic prefix. The GP has to be sufficiently long to accommodate the propagation delay and the hardware switching time to properly enable the DL/UL transition.

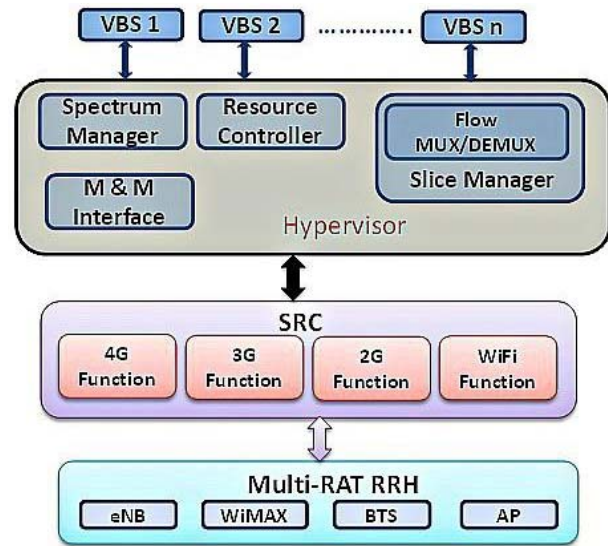


Fig. 1. Block diagram of a multi-RAT SBS.

III. LOCALLY VIRTUALIZED NETWORK (LVN)

We propose the LVN as a distributed virtualization model that consists of virtualized BSs distributed in a certain coverage zone. In this model, BSs are virtualized (or sliced) to create multiple VBSs that are operated by different VNOs. A flow-based virtualization method is adopted, where the incumbent VBSs in a physical BS are isolated at the flow-level. The virtualization models in [6], [8], and [9] require modifications to the existing network nodes and use of a separate IT-based network in order to implement virtualization functionalities. But the LVN model proposed in this paper uses a single network substrate composed of SBSs to implement VBSs. We use OpenFlow [28] for flow-level virtualization of the physical BSs; we also consider that the nodes in LVN are multi-RAT capable. A detailed description of the LVN model is given in this section along with its dimensioning and cost analysis.

A. LVN Architecture

For the LVN framework, we propose a BS architecture that is an enhanced version of multiple radio access technology (multi-RAT) enabled BS [29] with hardware augmentation (by including a hypervisor module) to make them virtualization-capable. We refer to these newly created base stations as super base stations (SBSs). The multi-RAT SBSs are capable to support multiple wireless access technologies (e.g., WiFi, 3G, OFDMA based 4G systems, etc.) simultaneously to serve user equipments (UEs) using one or some if not all of these RATs. The major enhancement in the SBS architecture (cf. Fig. 1) is the ‘Hypervisor’ block, which virtualizes (or slices) the physical SBS into multiple virtual BSs (VBSs). Traditional BSs are operated by a single operator; hence, all the hardware (processing, storage, transmission, etc.) and radio resources are exploited and managed by that operator. On the contrary, an SBS is sliced into multiple virtual BSs (VBSs), each of which belongs to a different network operator. The hypervisor in the SBS is in fact, the virtualizing entity that manages isolation

among the incumbent VBSs and provisions hardware and radio resources among them according to the service level agreement (SLA) between the virtual network operators (VNOs) that operate the VBSs and the infrastructure provider (InP), which is responsible for deployment and management of the SBSs.

The hypervisor consists of four components: a resource controller, a spectrum manager, a slice manager, and a management and monitoring (M & M) interface (cf. Fig. 1). The resource controller keeps track of the resources of the SBS and collaborates with the slice manager for proper resource provisioning. Specialized software libraries (SLs) are used to handle the resource allocation for each RAT. For example, the SL for OFDMA-based networks (LTE, WiMAX) assigns physical resources at the granularity of physical resource blocks (PRBs) of the OFDMA frame structure. Similarly, for other incumbent RATs, the corresponding SLs will partition resources depending on the underlying PHY and MAC layer technologies. The spectrum manager, which orchestrates air interface virtualization is basically a spectrum allocation entity that provides radio resources to the VBSs according to their need and corresponding SLAs.

The VBSs residing in the physical SBS need to be functionally isolated from each other, so that, the operation of one does not interfere with the other. As such, the VNOs operating the VBSs should do so in a way equivalent to possessing a physical base station themselves. This is provisioned by the slice manager that isolates the incumbent VBSs in flow-level. Traffic flow from the VBSs in the downlink (DL) direction is intercepted by the hypervisor and the slice manager decides which RAT module in the SRC unit this flow should be sent to. Slice-IDs are used to distinguish flows from different VBSs. Similarly, in the uplink (UL) direction, traffic flows coming from the SRC are checked for the slice-ID by the slice manager to decide on their destination VBS and directs the flow to the appropriate VBS. The flow multiplexing/demultiplexing unit in the slice manager is responsible for the flow management in the DL and UL directions. The slice manager does the flow level virtualization [30]. For proper management of the wireless access, a VNO needs to monitor the state of its nodes and act if any change is needed. This functionality is provided by the M&M application programming interface (API) of the hypervisor.

The hypervisor interacts with the single radio controller (SRC) [29], which is a unified network controller for multi-standard radio resource management. As we can see from Fig. 1, the SRC has 4G, 3G, 2G, and WiFi function modules which manage the corresponding transceiver units at the multi-RAT RRHs. The core network can be virtualized as described in Section IV.

B. LVN Dimensioning

Let the number of operators in area A be n_{op} . Assuming the number of slices per SBS, n_{sl} , the required number of SBSs in area A is,

$$N_{SBS} = \frac{n_{op}}{n_{sl}} \times \max\left(\frac{A}{\pi \times d_{sbs}^2}, \frac{N_{ue} \times R_{ue}}{R_{SBS}}\right) \quad (11)$$

where d_{sbs} is the coverage radius of a SBS. In our network planning, we deploy macro-SBS in the coverage-limited case, whereas smaller (micro and pico) cells are deployed in the capacity-limited case according to traffic demand in specific places (e.g., hotspots).

C. LVN Cost Analysis

Since the SBS is basically an augmentation of a traditional BS, we adopt its cost as a reference value when calculating the SBS cost. We suppose that the cost of every SBS increases by γ ($=20\%$) with each extra slice its houses. This is just a simplified assumption to account for the economies of scale made possible by SBS resource sharing. So, the cost of the SBS radio equipment is

$$C_{eq_i}^s = C_{eq_i} \times [1 + \gamma \times (n_{sl} - 1)] \quad (12)$$

where C_{eq_i} is the cost of a traditional BS at tier i , n_{sl} is the number of slices in a SBS. Expenditures for site build out, site leases, power consumption and O&M are approximated in a similar fashion. Hence, the total cost per tier is

$$C_i^l = N_{SBS_i} \times (C_{cap_i}^l + C_{opi}^l) \quad (13)$$

where N_{SBS_i} is the total number of SBSs in tier i , C_i^l is the total cost for tier i , $C_{cap_i}^l$ and C_{opi}^l are the corresponding CAPEX and OPEX, respectively, for a SBSs in tier i . Further, the CAPEX can be expressed as

$$C_{cap_i}^l = C_{eq_i}^s + C_{sbi}^s \quad (14)$$

where $C_{eq_i}^l$ and C_{sbi}^s are the equipment and site-build cost, respectively. And the OPEX can be decomposed as

$$C_{opi}^l = C_{sri}^s + C_{omi}^s + C_{bhi}^s \quad (15)$$

where C_{sri}^s , C_{omi}^s and C_{bhi}^s are the site-rent, operation & maintenance (power consumption and maintenance), and backhaul costs, respectively. Hence, the total cost for the LVN is

$$C_T^l = \sum_{i=1}^K C_i^l. \quad (16)$$

We use the *cumulated discounted cash flow* method to calculate the total cost per tier i in present time. If, on average, one BS is exploited for Y years, then for a discount rate d , the total cost can be calculated as

$$\begin{aligned} C_{DT}^l &= \sum_{y=0}^{Y-1} \frac{C_T^l}{(1+d)^y} \\ &= \sum_{y=0}^{Y-1} \frac{\sum_{i=1}^K C_i^l}{(1+d)^y}. \end{aligned} \quad (17)$$

IV. CLUSTERED/REMOTE VIRTUALIZED NETWORK (CVN/RVN)

The CVN/RVN is a cloud-based virtualization framework. In this model, computing, storage and networking resources are pooled in wireless data centers that we refer to as central processing centers (CPCs). In a CPC, BS functionalities are

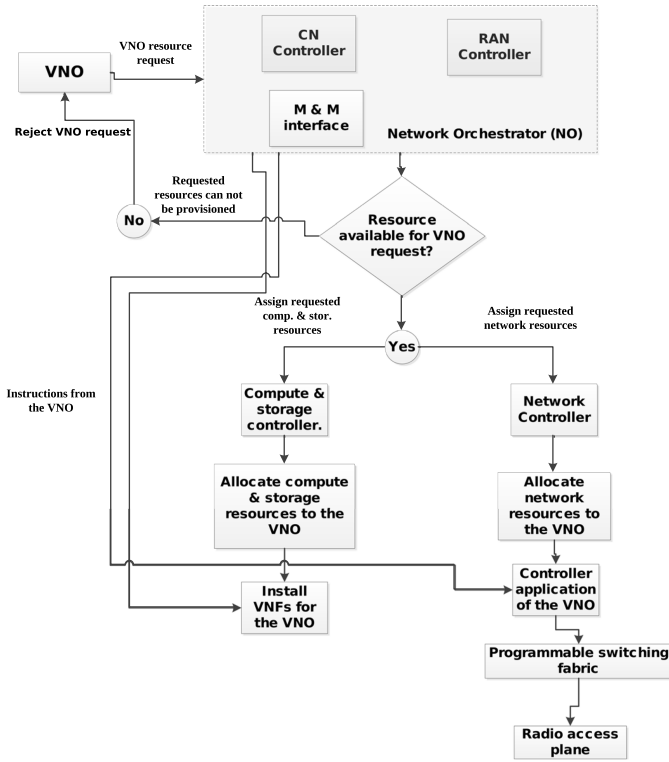


Fig. 2. Flow chart showing a NO's decision steps.

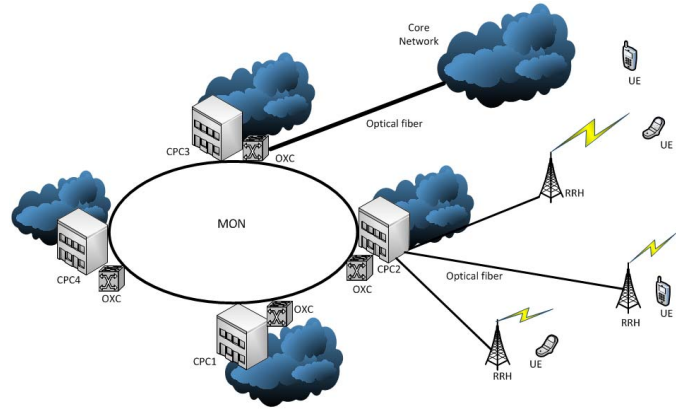


Fig. 3. CVN Architecture.

implemented as software instances on IT-grade servers and radio access is provided via fiber-connected, distributed and multi-RAT RRHs. When a single *large* CPC is used to cover a certain geographical area *A*, we refer to this network as a remote virtualized network (RVN). When a number of *smaller* CPCs are distributed to cover the area *A*, the network is called a clustered virtualized network (CVN). A typical CVN architecture is shown in Fig. 3 that consists of distributed data centers interconnected by a metropolitan optical network (MON) which is composed of optical cross connects (OXCs) and fiber optic cables. We advocate the use of SDN and cloud computing as enabling technologies for implementing the proposed CVN/RVN model. By separating the control and data planes, SDN enables network programmability and innovative service provisioning in otherwise closed telecommunication networks. Resource sharing as well as elastic and on-demand resource provisioning are possible in the new cloud computing paradigm. There are mainly three parts in this architecture: the Network Orchestrator (NO), the Radio Access Network (RAN) (cf. Fig. 4), and the Core Network (CN) (cf. Fig. 5). We discuss the detailed architectural components of the CVN/RVN framework in this section. We also present the dimensioning of a CVN/RVN network that follows with the cost analysis of this model.

A. Network Orchestrator (NO)

The NO is the central control point for both the access and core networks. It controls the underlying physical and virtual resources. It consists of both RAN and CN controllers. It also provides a configuration & monitoring interface to

the VNOs and SPs. Each VNO has a network controller that manages the underlying SDN-based network fabric. The compute & storage controller manages the computing and storage resources. The conventional NO is motivated by the SDI resource management system in [13], which is used to control and manage the underlying networking & computing resources in a wired network environment. The flow-chart in Fig. 2 shows the various steps involved in the NO's decision making in the creation and subsequent operation of VNOs. A prospective VNO requests its required resources from the NO (managed by an InP). The NO consults its resource database to see if the VNO's request can be satisfied. If resources are insufficient, it would notify the VNO that its request cannot be fulfilled. But if the InP has available resources to satisfy the VNO's demand, the compute & storage controller of the NO will allocate these resources to the VNO. The VNO can then install its virtual network functions (VNFs) (e.g., switching gateway (SGW), packet data network gateway (PGW), mobility management entity (MME), etc. for a MVNO case) in the allocated memory locations. Similarly, the network controller unit of the NO assigns network resources in accordance to the VNOs request. The VNO can build its customized network using its own network controller application that programs the underlying programmable switching and radio plane devices. Hence, a VNO has its own network consisting of VNFs and a virtual network.

B. Radio Access Network (RAN)

The CVN/RVN RAN consists of the network fabric and the compute & storage parts. A detailed network diagram is shown in Fig. 4. This section describes these platforms in detail.

1) *Network Fabric:* The network fabric consists of programmable switches and radio devices (RRHs) that can be programmed following the SDN paradigm. A virtual network operator (VNO) or service provider (SP) can build its own customized network in the networking fabric by programming its allocated network resources. VNOs express the functional behavior of their networks by different SDN applications. The controller platform (e.g., POX [31], NOX [32], Ryu [33], FloodLight [34], etc.) converts the high level network policies from the application layer and expresses them in a

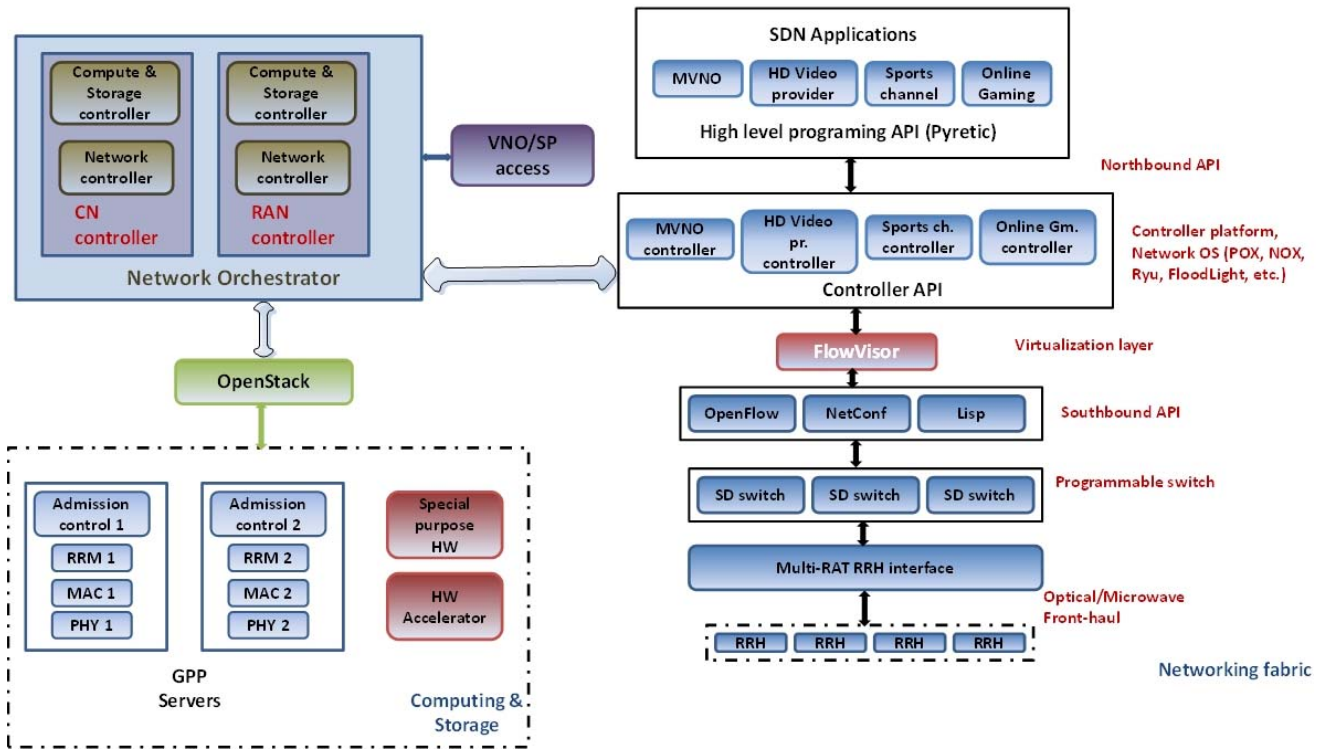


Fig. 4. Functional block representation of a CVN/RVN RAN with a network orchestrator.

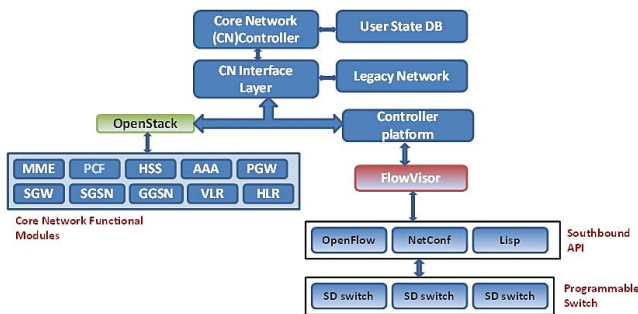


Fig. 5. CVN/RVN core network flow diagram.

form compatible with the underlying programmable switching fabric. For this purpose, the controllers use a southbound API, e.g., OpenFlow [28] to modify the forwarding behaviour of underlying switches. A multi-RAT interface layer (ADC/DAC) translates the information to the appropriate RAT by the optical (or microwave) front-haul.

For virtualizing the network fabric, a controller (e.g., FlowVisor [30]) is used which is basically a transparent proxy that ensures isolation among the virtual operators (SDN applications). Different SDN applications (e.g., VNO, HD video provider, sports channel provider, gaming companies, etc.) can be built using a high-level network programming API (e.g., Pyretic [35]). Domain-specific programming languages like Pyretic are programmer-friendly, provide high-level network abstraction, and enable a programmer's task of writing modular network applications.

2) *Compute & Storage Unit*: The network applications and various signal processing software components are stored and executed in the compute & storage unit. The compute & storage controller takes the high-level requirements from third parties (e.g., MVNOs and SPs) and allocates computing, storage and radio resources. For such an “infrastructure as a service (IaaS)” deployment, we have used the open source cloud computing platform, OpenStack [36].

Current heterogeneous multi-RAT technologies use different PHY and MAC layer and radio resource management (RRM) functions. To facilitate the development of customized RAT technologies, different PHY, MAC and RRM techniques are implemented as individual software modules in GPP servers (see bottom-left part in Fig. 4). As such, any VNO or SP can combine different modules that efficiently implement its intended service & application. A VNO can also develop its own customized PHY, MAC or RRM protocols. For demanding PHY-layer processing features, special purpose hardware and hardware accelerators are used.

C. Core Network (CN)

The CN is implemented in GPP servers using OpenStack [36] technology to enable the cloud computing paradigm. It has three main parts as illustrated in Fig. 5, an interface layer, user-state database (DB), and CN functional modules. The CN interface layer is a communication interface with the network controller that sends/receives network configuration instructions for the computing & storage and the networking sections. It also communicates control signals and data with legacy (non virtualized) network elements.

The user state DB compiles all state information for the users. Hence, the underlined virtual entities can be stateless.

The core network control-plane functions such as the mobility management entity (MME), the policy & charging rule function (PCRF), the home subscriber server (HSS), the authentication, authorization & accounting (AAA), etc. are implemented as software modules. As such, the VNOs/SPs can create their (virtual) components for the respective service provisioning. For data-plane forwarding, FlowVisor [30] virtualizes the underlined software-defined programmable switch fabric.

The CVN/RVN model proposed here uses software instances of BSs implemented in servers with distributed fiber-connected RRHs and OpenFlow [28] for virtual wireless access rendering. It also provisions for multi-RAT RRHs. In contrast, the model in [10], considers VBS pooling over two servers only and does not analyze the more realistic case when the scale of VBS pooling becomes as large as that of a data center. Also the work in [10] does not address critical virtualization issues like slice isolation and customized network stack implementation capabilities for VNOs. Moreover, unlike the proposed CVN/RVN model, the C-RAN architecture in [17] does not use OpenFlow [28]. As such the proposed OpenFlow-based [28] CVN/RVN architecture therefore accounts for the aforementioned features. And the radio signal transmission over fiber (RoF) actually becomes a critical issue for the implementation of large data center. The new CVN/RVN model takes into consideration the RoF issue and provides a guideline for wireless data center dimensioning, a key aspect that has not been studied in the open literature to the best of the authors' knowledge. From a broader perspective, we envision the distributed CPCs as a "cloud of wireless data centers". As a proof of concept, a virtual heterogeneous wireless access network model was implemented by the authors of this work in [37] using an emulation platform, where service differentiation was studied for two virtual networks that were implemented in a common subset of network infrastructure. Emulation results suggested that virtual wireless networks are able to achieve the QoS requirement of carrier networks while ensuring efficient resource utilization by sharing a common subset of network infrastructure.

D. CVN/RVN Dimensioning

The required number of RRHs for macro-coverage can be calculated as

$$N_r^m = n_{op} \times \max \left(\frac{d_{cpc}^2}{\pi \times d_m^2}, (v_m \times (\mu_m \times A_{cpc}) \times R_{um}) / R_{MBS} \right) \quad (18)$$

where d_{cpc} and A_{cpc} are the CPC size and coverage area, respectively, and μ_m , v_m and R_{um} are the user density, the HetNet coefficient (i.e., the ratio of macro, micro and pico cells) and the average user data rate, respectively. Similarly, the number of RRHs for micro-coverage is

$$N_r^{mi} = (v_{mi} \times (\mu_{mi} \times A_{cpc}) \times R_{umi}) / R_{MiBS} \quad (19)$$

and the number of RRHs for pico-coverage is

$$N_r^p = (v_p \times (\mu_p \times A_{cpc}) \times R_{up}) / R_{PBS}. \quad (20)$$

Please note that the work in [10] dedicates two processor cores for the implementation of one macro VBS only. Since micro and pico cells serve lower loads than a macro cell, it is intuitive that the micro and pico base stations will require less processing hardware. From a "processor core" point of view, the required number of servers required for a CPC, considering servers with eight-core processors, can be calculated as

$$N_{ser} = (N_r^m \times pc_m + N_r^{mi} \times pc_{mi} + N_r^p \times pc_p) / 8 \quad (21)$$

where pc_m , pc_{mi} , and pc_p are the numbers of dedicated processor cores required for macro, micro, and pico VBSs, respectively. And N_r^m , N_r^{mi} , and N_r^p are the numbers of RRHs for macro, micro, and pico cell coverage in the concerned area. It is worth noting in our analysis that we assumed each cell to have its own dedicated RRH. The number of server racks is $N_{rack} = N_{ser} / N_{ser}^{rack}$, where N_{ser}^{rack} is the number of servers per rack. The number of switches and OXCs are approximated as $N_{sw} = N_{rack}$ and $N_{oxc} = N_{rack}$, respectively.

E. RRHs Cost

The RRH cost is calculated as

$$C_{rrh} = C_{rrhc} + C_{rrho} \quad (22)$$

where C_{rrhc} and C_{rrho} are the RRHs' CAPEX and OPEX, respectively. C_{rrhc} consists of the radio equipment (c_{rrhe}) and the site installation costs (c_{rrhsi}). Whereas the OPEX consists of O&M costs only. No site lease nor backhaul costs are considered for the RRHs since fiber optic cables are used for radio signal transmission. Hence, the RRHs' cost in a CPC is

$$C_{rrh} = N_r^m \times C_{rrh}^m + N_r^{mi} \times C_{rrh}^{mi} + N_r^p \times C_{rrh}^p \quad (23)$$

where C_{rrh}^m , C_{rrh}^{mi} , and C_{rrh}^p are the separate RRHs' costs for macro, micro and pico coverage, respectively. The cumulated discounted cash flow for the RRHs over Y years is calculated as

$$C_{rrh}^t = \sum_{y=0}^{Y-1} \frac{C_{rrhy}}{(1+d)^y} \quad (24)$$

where C_{rrhy} is the cost of the RRHs in year y .

F. CPC Cost

The CPC cost accounts for different expenditures that cover the data-center's occupied space, the power consumption for hardware (processing and cooling, the personnel salaries, software costs, etc. For real estate expenses, we adopt the following model proposed in [38].

1) *Space Cost*: The real estate value for a CPC per year can be calculated as [38]

$$C_{sp} = \frac{NOI \times A_{cpc} \times oc}{CP} \quad (25)$$

where NOI is the net operating income per square meter per year, CP is the capitalization rate, A_{cpc} is the CPC area and oc is its occupancy factor.

2) *Power Delivery Cost*: A power delivery system in a typical data center is expected to feed air conditioning, battery back-up, on-site power generation, and both delivery and generation redundancies. Depreciation or amortization and maintenance costs are associated with the infrastructure that encompasses all the aforementioned functions. Hence, the cost burden of power delivery per year can be expressed as [38]

$$C_{pwr} = (1 + K_p) \times c_e \times P_{HW} \quad (26)$$

where c_e is the cost of power delivery per watt per year, P_{HW} is the hardware power consumption, and $K_p = J \times C_{am}^{pwr} / c_e$ is the power burden factor where J is the capacity utilization factor and C_{am}^{pwr} is the amortization & maintenance cost per watt per hour.

3) *Cooling Cost*: The cooling cost can be estimated as [38]

$$C_{col} = (1 + K_c) \times L \times c_e \times P_{HW} \quad (27)$$

where K_c is the cooling burden factor and $L = \frac{P_{cooling}}{P_{HW}}$ is the load factor.

4) *Personnel Costs*: Let the number of personnel per rack in a data center be composed as follows: IT technicians H_{IT} , facility service employees H_f , and administrative clerks H_a . If the average yearly salary is C_{ap} , then the personnel costs per year can be calculated as [38]

$$C_{per} = (H_{IT} + H_f + H_a) \times C_{ap} \quad (28)$$

5) *Software Cost*: The software cost for a data center is

$$C_{sofw} = N_{rack} \times C_{swr} \quad (29)$$

where N_{rack} is the total number of racks in the data center and C_{swr} is the average yearly cost of software and licenses per rack.

6) *IT Equipment Cost*: IT equipment consists of servers, switches, and OXC. Their cost for a CPC is calculated as

$$C_{IT} = N_{rack} \times C_{rack} + N_{sw} \times C_{sw} + N_{oxc} \times C_{oxc} \quad (30)$$

where N_{sw} is the number of switches, N_{oxc} is the number of OXCs, and C_{rack} , C_{sw} , and C_{oxc} are the unitary costs of servers per rack, switches, and OXCs, respectively.

7) *Optical-Fiber Deployment Cost*: The optical-fiber deployment cost is expressed as

$$C_{fb} = (C_f \times L_{af} + C_{tr}) \times N_{tot}^{rrh} \quad (31)$$

where C_f is the fiber cost per km, L_{af} is the average optical fiber length, C_{tr} is the cost of an optical transponder, and N_{tot}^{rrh} is the total number of RRHs.

8) *Total CPC Cost*: The CAPEX of a CPC is

$$C_{cap}^{cpc} = C_{fb} + C_{IT} \quad (32)$$

whereas its OPEX is

$$C_{op}^{cpc} = C_{sp} + C_{pwr} + C_{col} + C_{per} + C_{sofw} \quad (33)$$

Hence, its total cost is

$$C_{cpc} = C_{cap}^{cpc} + C_{op}^{cpc} \quad (34)$$

TABLE III
RRH PARAMETER

Parameter	MBS	MiBS	PBS
Cell range (R)	700 m	175 m	70 m
Capacity (W_{BS})	300 Mbps	100 Mbps	100 Mbps
Radio equipment cost [\$k]	10	4	0.1
Site build-out [\$k]	-	-	-
Site installation [\$k]	5	2	0.5
Annual O&M [\$k/year]	0.3	0.1	0.1
Annual site lease [\$k/year]	-	-	-
Annual transmission [\$k/year]	-	-	-

TABLE IV
CPC COST PARAMETER

Parameter	Cost [\$k]
Server	11
Switch	8
OXC	10
Fiber optic cable	0.01/unit area
Site buildout	100
Site installation	40
Annual O&M	5
Annual site lease	15
Annual transmission	0

and its cumulative discounted cost is

$$C_{cpc}^t = \sum_{y=0}^{Y-1} \frac{C_{cpcy}}{(1+d)^y} \quad (35)$$

where C_{cpcy} is the CPC cost in year y . The total cost for a CPC network, including its distributed RRHs, is therefore calculated as

$$C_{cpc}^T = C_{cpc}^t + C_{rrh}^t \quad (36)$$

G. Total CVN/RVN Cost

The number of CPCs is $N_{cpc} = A_{rgn} / A_{cpc}$, where A_{rgn} is the area covered by the network and A_{cpc} is the coverage area of a CPC. Hence the total CVN/RVN cost is

$$C_n^{c/r} = N_{cpc} \times C_{cpc}^T \quad (37)$$

The itemized cost values of the RRHs and CPC nodes, inspired from [22] and [38], respectively, are listed in Tables III and IV. Please note that the RRHs do not incur any noticeable costs for their site build-out and lease or for their baseband signals' transmission. Also please note that the costs for the CPC nodes were properly set after careful consultation of different vendor websites and that the costs of real estate, power consumption, and other items were approximated by representative values [38].

H. Proof of Concept Implementation

As a proof of concept, we have implemented two VNOs in the Mininet [39] emulation platform. These VNOs are implemented as two isolated slices sharing the same physical resources, e.g. computing & storage nodes, network switches, RRHs, etc. The schematic of the emulation structure is shown in Figure 6. In the emulation setup, VNO1 is a MVNO

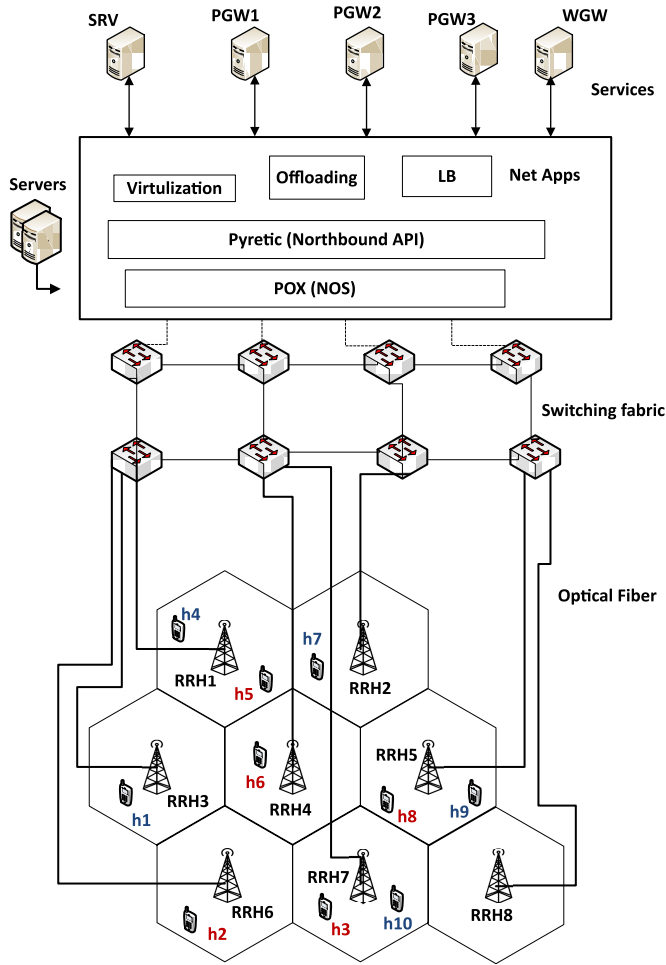


Fig. 6. Virtual wireless networks emulation scenario.

that provides mobile network services to its customers and VNO2 is an internet service provider (ISP), providing wireless internet access to users through unlicensed spectrum. We envision a NFV implementation for the operators, where various network processing nodes, for example, packet gateway, mobility management unit, baseband processing nodes, etc., are implemented as software instances in the CPC. In the emulation scenario (Fig. 6), the processing nodes labelled ‘SRV’, ‘PGW1’, ‘PGW2’ and ‘PGW3’ belongs to the VNO1 and the processing node ‘WGW’ is a VNO2 element.

In this experiment, we have studied service differentiation provisioning for virtual wireless networks in a CVN/RVN model. We study how various mobile services can be provided with differentiated QoS depending on the application requirement and also the user subscription category. More specifically, we studied load balancing for users of VNO1 that have different subscription categories (prioritized and normal) and also the offloading of delay tolerant traffic from VNO1 to VNO2. As performance metrics, we measure round trip transmission delay (RTTD) and achievable throughput while implementing the traffic offloading and load balancing. Network applications, i.e., virtualization (slicing), offloading and load balancing are written using a domain specific programming language (DSPL) named Pyretic [35], which is a northbound

API. The SDN controller platform POX [31] was used which is a Python programming language based network operating system (NOS). POX uses OpenFlow [28] as the southbound API to modify the forwarding tables of the underlying programmable switches (i.e., open virtual switches (OVSS) [40]) to forward traffic from the respective VNOs. RRHs were connected to the CPC via high capacity optical fiber cables.

VNO1 operates in licensed radio spectrum while VNO2 uses unlicensed spectrum. Varied radio link qualities for the two types of networks are realized by implementing more lossy links for the WiFi network. From a QoS point of view, VNO1 guarantees better service quality via its dedicated licensed spectrum and high performance servers connected by high capacity network links. As shown in Fig. 6, users h2, h3, h5, h6 and h8, marked red, belong to VNO1, where h2 and h3 are corporate users who enjoy better network services due to their higher subscription category and h5, h6 & h8 are regular users. Users h1, h4, h7, h9, h10, marked in blue, are served by VNO2. In the wireless data center, connections between the servers and switches are of 1GB capacity, while no transmission delay and loss are assumed for these links. The server hosting PGW2 VM (for serving regular clients from VNO1) is connected via a 800 MB link having a 2% packet loss, while for the WGW VM (to serve delay-tolerant traffic), the link is 600 MB, with 0.5 ms delay and a 2% packet loss. These links are configured in such a manner so as to simulate a differentiated QoS. Connections between switches and between switches and RRHs are of 1GB capacity. The fiber length from WDC to the RRH is 2 km, hence a 0.01 ms of transmission delay is assumed, as typical delay for radio transmission over optical fiber is $5\mu\text{s}/\text{km}$.

Users of VNO1 have simultaneous access to both the mobile network and the WiFi network. Given the omnipresence of WiFi networks in our everyday ICT eco-system, e.g. WiFi networks in campuses, offices, shopping malls, airports, stadiums, etc., it is a reasonable assumption. For the service differentiation evaluation, delay sensitive traffic (e.g. file transfer, video streaming, etc.) from the users of VNO1 directed to PGW1 (default server for data traffic for the UEs of VNO1) are offloaded to the WGW server, that belongs to the VNO2. This helps save licensed spectrum that can be used for providing services having tighter QoS requirements, e.g. services producing more delay-sensitive traffic. Also, in case of VNO1, traffic from privileged users (h2, h3) is directed to server (PGW3) capable of providing better QoS from achievable throughput and RTT delay point of view. Table V shows the RTT delay and throughput for different service differentiation cases, when the users are static.

RTTD are measured in ms and the throughput in Mbps. The ‘Regular’ column shows delay and throughput when traffic from users is forwarded to the server ‘SRV’. The ‘Offloading’ is the measure when delay-tolerant traffic from VNO1 is offloaded to VNO2 and the ‘Load balancing’ shows the result of differentiated services for privileged (h2, h3) and regular (h5, h6, h8) users. Minimum and average delays are shown in the table. For the control information exchange between the controller and switches, the transmission time for the

TABLE V
DELAY AND ACHIEVABLE THROUGHPUT FOR STATIC USERS

UE	Regular		Offloading		Load balancing	
	RTTD [min - avg]	Th [MB]	RTTD [min - avg]	Th [MB]	RTTD [min - avg]	Th [MB]
VNO1 cor. users	0.2 - 46	95.2	1.6 - 11	27.3	0.12 - 35	95.7
VNO1 reg. users	0.36 - 28	94.7	1.32 - 12	28.8	0.21 - 39	79.8
VNO2 users to SRV	0.36 - 51	31.2	-	-	-	-
VNO2 users to WGW	1.45 - 50	10.3	-	-	-	-

TABLE VI
DELAY AND ACHIEVABLE THROUGHPUT FOR MOBILE USERS

UE	Regular		Offloading		Load balancing	
	RTTD [max - avg]	Th [MB]	RTTD [max - avg]	Th [MB]	RTTD [max - avg]	Th [MB]
VNO1 cor. user before hand- over	1931 - 148	94.8	919 - 48	23.9	775 - 39	95.7
VNO1 cor. user after hand- over	1738 - 129	95.0	794 - 44	29	924 - 47	95.6
VNO1 reg. user before hand- over	1989 - 156	94.9	894 - 47	27.9	802 - 43	78.4
VNO1 reg. user after hand- over	2457 - 221	95	518 - 28	25.9	750 - 40	79.7
VNO2 user before hand- over	2142 - 172	35.5	-	-	-	-
VNO2 user after hand- over	1429 - 97	34	-	-	-	-

first packet is quite high which in turn increases the average packet delay; in fact, the long term average delay is lower than the noted average delay in Table V. No offloading or load balancing is assumed for VNO2, as shown in Table V. Services provided by WiFi ISPs are of *best effort* type, for this reason, VNO2 does not require traffic offloading or load balancing. We implemented a random mobility model for the users of VNO1 and VNO2, and Table VI shows the maximum (for the first packet) and the average packet RTTD, including

the average achieved throughput when the users are nomadic. The delay depends on the connected RRH and the quality of links to the service nodes. According to the 3GPP standard, the preferable delay for LTE voice and video is <150 ms and the maximum allowable delay is <400 ms. From the average RTTD values in Table V and VI, we can see that the CVN/RVN model satisfies these requirements very well.

V. HYBRID VIRTUALIZED NETWORK (HVN)

The HVN framework is a combination of the LVN and CVN/RVN models. It consists of CPCs as well as selectively-distributed SBSs. The cost advantages of the CVN/RVN depend on application-specific QoS penalties that impose minimum acceptable thresholds. To alleviate this problem, a HVN, which is basically a combination of a LVN and a RVN, offers the best cost vs. QoS trade-offs. Indeed, a HVN deploys data centers with SBSs distributed in the coverage area to meet the service requirements of delay-sensitive traffic. As one example, suppose that a data center of either RVN or CVN type covers a certain metropolitan area. And assume that there are many offices in the downtown of that metropolitan area that generate a significant amount of voice and live-video traffic during office hours. A data center with distributed RRHs might not be able to cope with this highly delay-sensitive traffic demand. To alleviate this problem, a number of SBSs can be distributed throughout the downtown area in order to handle the delay-sensitive traffic (e.g., voice, live video, etc.) and off-load the more delay-tolerant traffic (e.g., text, file transfer, web browsing, video streaming, etc.) to the data center. A network designer has to take into consideration the demography and expected traffic patterns of any given deployment area and specify a HVN that is able to handle the traffic QoS demand in the most efficient way. A HVN model can be expressed in terms of weights as

$$HVN = p_c \times RVN + (1 - p_c) \times LVN \quad (38)$$

where p_c is the portion of the HVN that exploits a data center (i.e., the CVN/RVN part) and $(1 - p_c)$ is the remaining portion of the network that exploits SBSs (i.e., the LVN part).

VI. DATA RATE AND UTILITY FUNCTION CONSTRUCTION

The virtualization frameworks presented in the previous sections are quite different in terms of their underlying network structure and hardware choices. Hence, they have their relative pros and cons as far as the network cost, energy efficiency [41], and QoS are concerned. As one example, using IT-grade network equipment in a CVN/RVN architecture is more cost efficient than using SBSs in a LVN framework. But carrying signals over RoF from a CPC to the RRHs (and vice-versa) has its own challenges and limitations from a QoS point of view. To investigate the trade-offs between a network operator's budget and the service quality requirements of the intended service, we have developed an analytical model for the proposed virtualization frameworks. This model considers both network cost and QoS (achievable data rate) as well as the operator's preference for cost effectiveness and service quality of the network. In our analysis, we have only considered

single-RAT multi-tier networks for the sake of simplicity and conciseness. The most general multi-RAT multi-tier HetNet case is under investigation and will be the subject of a future publication. We have also considered LTE-TDD downlink transmission. The granularity of physical resources is adjusted down to the level of the physical resource block (PRB) of the OFDMA frame structure. The data rate for an OFDMA system can be calculated as [42]:

$$R_{TDD} = \frac{N_{sub} \times N_{mod} \times N_{cod}}{[N_{FFT}/(n \times BW)](1 + G)} \quad (39)$$

where N_{sub} is the number of data subcarriers and N_{mod} and N_{cod} are the numbers of modulated bits per symbol and the coding rate, respectively. BW , n , and G are the operating bandwidth, the sampling factor, and the cyclic prefix length, respectively.

In a TDD system, maintaining time synchronization between the uplink and downlink transmissions is critical. The lack of synchronization can disrupt proper decoding of the transmitted information. In the CVN/RVN framework, this issue is more critical since the radio propagation path involves the whole span of optical fiber between the RRHs and the CPC. The time slot in an OFDMA subframe that enables this time synchronization is called the guard period (GP). In our design, we utilize this GP to accommodate the transmission delay for carrying radio signal over the optical fiber cables that spans from the CPCs to the RRHs. The data rate for such an OFDMA system employing RoF transmission can therefore be expressed as

$$R_{TDD}^* = \frac{N_{sub} \times N_{mod} \times N_{cod} \times (T_{sf} - t_{enb} - d_{cpc} \times l)}{[N_{FFT}/(n \times BW)](1 + G) \times T_{sf}} \quad (40)$$

where T_{sf} is the length of the special sub-frame, t_{enb} is the switching time of the eNB, and d_{cpc} is the coverage size the CPC, and l is the latency per km for radio transmission in the fiber. To avoid over/under provisioning, we have adopted in our analysis a square shape for both total coverage and the CPC areas.

The extra delay incurred by transmissions over the optical fiber in the transmission causes losses in the achievable *goodput*. We characterize this error as the frame error rate (FER)

$$FER = \exp(-\alpha \times \sqrt{\delta}) \quad (41)$$

where $\delta = \frac{14-GP}{14}$ is the ratio of the pilot-bearing symbols to the total number of symbols in a OFDMA sub-frame and α is a parameter that models in a simple way the severity of the channel by the degradation rate at which identification and synchronization errors increase and, hence, the throughput decreases through the negative impact of a lower pilot to sub-frame ratio δ . This parameter should depend on most of the PHY-layer parameters like the channel bandwidth, the SNR, the modulation, the coding rate, etc. Taking into account the $\overline{FER} = 1 - FER$, the data rate in equation (40), referred to here as R_{LTE} since we consider here LTE HetNets,

reduces to

$$R_{LTE} = \frac{N_{sub} \times N_{mod} \times N_{cod} \times (T_{sf} - t_{enb} - d_{cpc} \times l)}{[1/(n \times \frac{BW}{N_{FFT}})](1 + G) \times T_{sf}} \times \overline{FER}. \quad (42)$$

Higher FER not only further degrades QoS uniformly across all types of users by reducing spectrum efficiency, but will further impact it, yet unequally, i.e., more so over delay-sensitive links, by increasing requests for packet retransmissions. While we account for the former effect on QoS, we do not for the latter's. As such, our data rate term should be properly modified to render both impediments. One way to do so is to redefine it as follows:

$$R'_{LTE} = p_s \times R_{LTE}^{1/e_s} + p_v \times R_{LTE}^{1/e_v} + p_{sd} \times R_{LTE}^{1/e_{sd}} + p_{id} \times R_{LTE}^{1/e_{id}} \quad (43)$$

where p_s , p_v , p_{sd} , and p_{id} denote percentages (i.e., positive values less than 1) of speech (or voice), video, delay-sensitive, and delay-insensitive links, respectively, i.e., we have

$$p_s + p_v + p_{sd} + p_{id} = 1$$

and where e_s , e_v , e_{sd} , and e_{id} denote the delay-severity impact exponents for speech, video, delay-sensitive data, and delay-insensitive data links, respectively.

Now, we formulate the multi-criteria network utility function that is composed of network cost and achievable data rate. Network operators should be able to express their preference in terms of level of importance to network cost (both CAPEX and OPEX) or QoS (data rate). This preference indicates how important one criterion is against the other in the framework selection process. Since network cost and QoS are not compensatory in the selection of a particular framework, the nullity and unity of the utility function is important [43]. For this reason, we compose the network utility as the geometric product of the normalized network cost and QoS gains:

$$U_{opt}(args1) = \max_{args2} [U(args)] = \left(\frac{C_{max} - C}{C_{max}} \right)^{w_c} \times \left(\frac{R'_{LTE}}{R_{LTE}^{max}} \right)^{(1-w_c)} \quad (44)$$

where w_c and $(1 - w_c)$ are the cost and data-rate weights, respectively, and $args2 = d_m, d_{cpc}, \phi, v, BW, GP$, $args1 = other\ PHY\ and\ MAC\ layer\ parameters$, and $args = args1 \cup args2$. Also $C_{max} = \max_{(d_m, \phi, v)} C$ and $R_{LTE}^{max} = \max_{(BW, GP, d_{cpc})} R'_{LTE}$.

VII. RESULTS

The choice of a certain framework essentially is based on a given compromise between the corresponding network cost and the achievable QoS. The LVN can reduce cost to some extent but its implementation complexity increases due to the pooling of (virtual) network nodes and the introduction of a hypervisor. The CVN/RVN is the most cost-effective solution due to its usage of inexpensive general purpose IT hardware for baseband signal processing. But the inclusion of optical fibers in its network architecture places limitations on the

TABLE VII
EVALUATION SCENARIOS

Scenario	BW [MHz]	ϕ [km^2]	d_{MBS} [km]	HetNet [%,%,%]	α
1 (reference)	20	1000	0.7	[20,30,50]	1.4
2	10	1000	0.7	[20,30,50]	1.4
3	20	1000	0.5	[20,30,50]	1.4
4	20	1000	0.7	[100,0,0]	1.4
5	20	100	0.7	[20,30,50]	1.4
6	20	1000	0.7	[20,30,50]	3.0

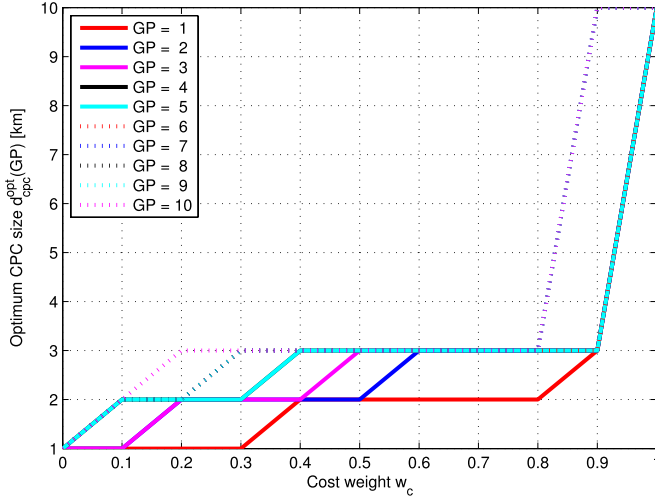


Fig. 7. Optimum CPC size $d_{cpc}^{opt}(GP)$ vs. cost weight w_c for different GP values in the reference scenario I (cf. Table VII).

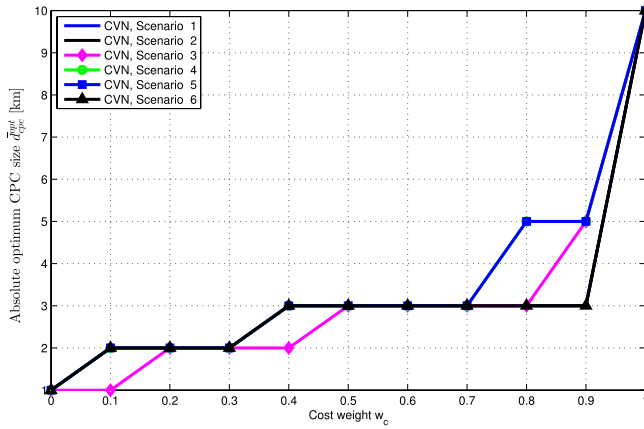


Fig. 8. Absolute optimum CPC size \bar{d}_{cpc}^{opt} vs. cost weight w_c in different scenarios (cf. Table VII).

achievable QoS due mainly to additional RTTD for radio transmission over fiber optic cables. The HVN is a more balanced approach to network cost and QoS optimization. In this section, we assess the impact of the PHY and the MAC layer parameters on the CPC size. We also investigate the impact of different wireless access configuration parameters on the achievable network utility performance.

A. Optimum CVN/RVN CPC Size d_{cpc}

The optimal size of a CPC depends on many parameters such as the system bandwidth, the coverage radius of the macro base stations, the network architecture (i.e., whether it is homogeneous or heterogeneous), etc. One of the most critical

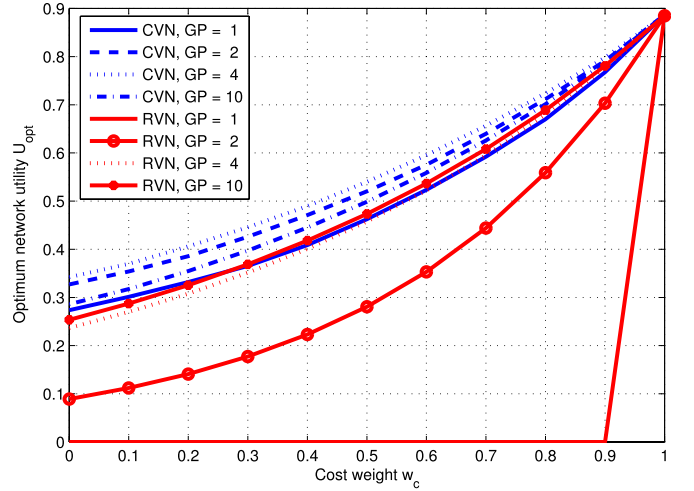


Fig. 9. Optimal network utility U_{opt} vs. cost weight w_c for different GP values in reference scenario 1 (cf. Table VII).

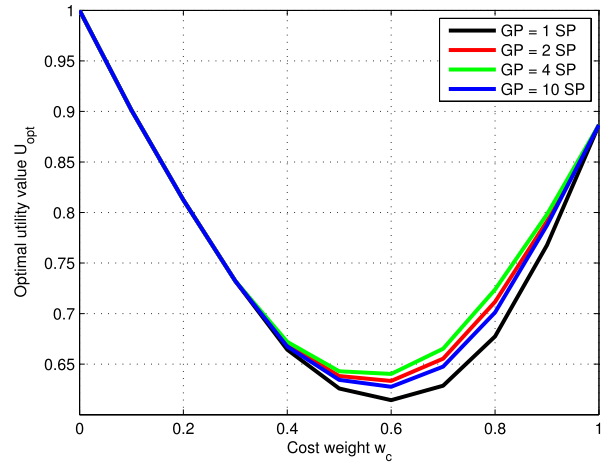


Fig. 10. HVN optimal network utility, U_{opt} , vs. cost weight w_c for different GP values in reference scenario I (cf. Table VII).

parameters affecting the CPC size is the GP value of an OFDMA subframe. Fig. 7 shows how the optimum CPC size d_{cpc}^{opt} versus the cost weight w_c varies with GP values in the reference scenario 1 of Table VII. When the primary concern is QoS (i.e., less emphasis on cost), smaller CPCs should be preferred. But when the operational budget is constrained, network designers should favor relatively larger CPCs with relatively wider coverage areas. A CPC of 1 to 3 km radius in a coverage area of 20 km radius is preferred for a wide range of w_c values. Interestingly, in the extreme case when there is no budget restriction (i.e., $w_c = 1$), the optimal CPC size is with a 10 km radius, meaning that a RVN (i.e., a single CPC covering the whole area) can never be an optimal design choice. It is worth mentioning that MAC layer parameters like GP can be optimized along with the cost-QoS trade-off in a CVN/RVN model. The severity of the transmission channel condition (modelled by α) impacts the optimal GP value GP_{opt} , i.e., when $\alpha = 1.4$, $GP_{opt} = 4$ symbol periods whereas for $\alpha = 3.0$, $GP_{opt} = 5$ symbol periods. For a coverage area with 20 km radius, the impact of different parameters (cf. different scenarios in Table VII) on the absolute optimal

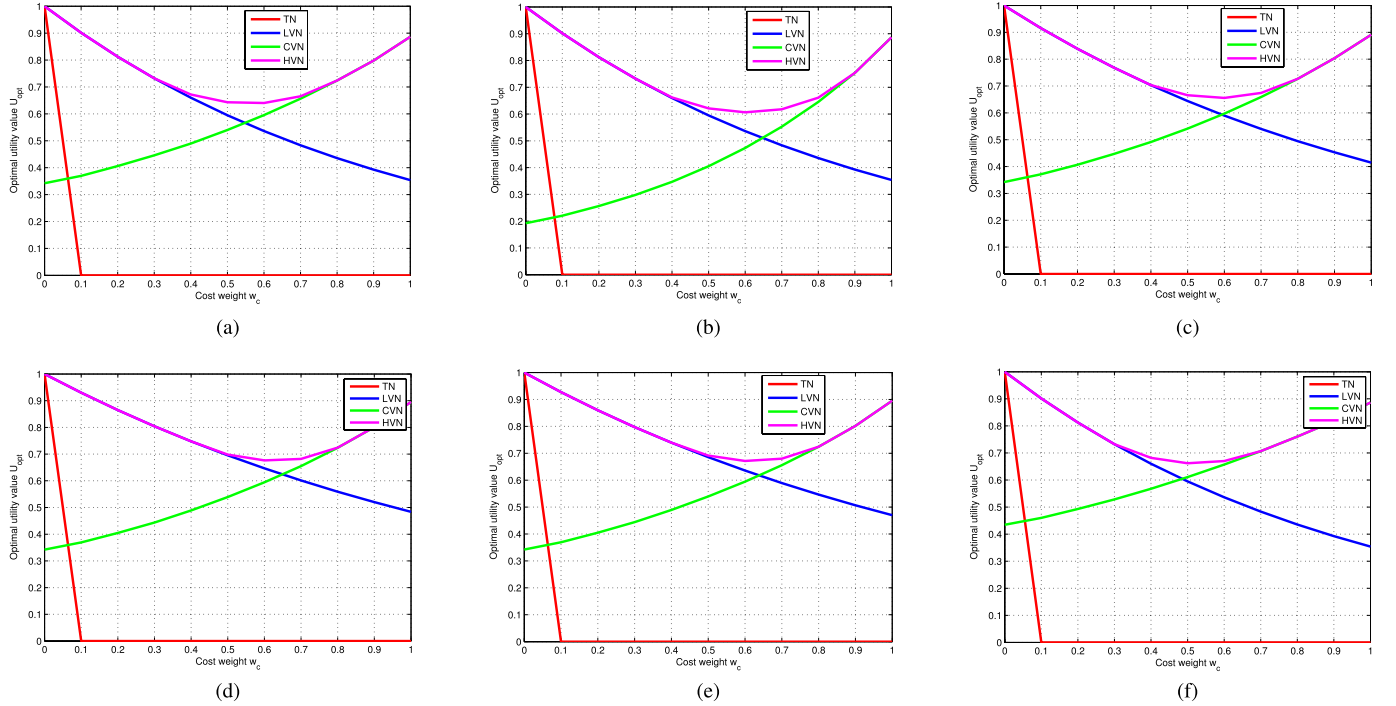


Fig. 11. Optimal network utility U_{opt} vs. cost weight w_c in different scenarios (cf. Table VII). (a) Scenario 1. (b) Scenario 2. (c) Scenario 3. (d) Scenario 4. (e) Scenario 5. (f) Scenario 6.

CPC size $\bar{d}_{cpc}^{opt} = d_{cpc}^{opt}(GP_{opt})$ (i.e., using optimized GP value GP_{opt}) is illustrated in Fig. 8.

B. CVN/RVN Utility U_{opt} at Different GP Values

The effect of GP on the total utility behaviour is also of prime importance. Fig. 9 shows the CVN/RVN utility behavior for different GP values in the reference scenario 1 (cf. Table VII). The CVN has better utility performance than RVN for some GP value. And the utility performance of both is worst for a $GP = 1$ symbol period. Indeed the optimal values of $d_{cpc}(GP)$ become relatively the smallest in this case (i.e., $d_{cpc} = 0.7$ km when $w_c = 0$), thereby increasing the network cost by a great extent. The maximum network utility is achieved with $GP = 4$ symbol periods (when $\alpha = 1.4$) because it balances both the cost and QoS in the most efficient manner. When $GP = 1$ in the RVN case, the network utility is severely penalized because just one symbol period is not large enough to account for radio propagation delays over a fiber distance of 20 km for adequate OFDM DL-UP synchronization. Hence the RVN architecture can never be a favorite choice, because the network's QoS is severely penalized due to the RVN's inability to properly resolve PHY (resolving transmission channel severity issues) and MAC (DL-UL synchronicity) layer issues.

C. Optimum Network Utility U_{opt} of HVN for Different GP Values

Fig. 10 illustrates the optimal network utility, U_{opt} , of a HVN network for different GP values. At lower cost weights, i.e., when $w_c \leq 0.4$, U_{opt} behavior is almost independent of the GP value variation. This is due to the fact that, in this

range of the w_c values, the dominant part of the HVN is composed of SBSs which do not incur any QoS degradation for RoF transmission delays, hence the invariance towards the GP value. But the interesting part of the graph is between $w_c = 0.4$ to $w_c = 0.8$, because in this design region, the HVN offers the most balanced trade-off between network cost and achievable QoS. This become more evident from the results of the following subsection.

D. Comparison of Optimal Network Utility U_{opt} for Different Frameworks

Fig. 11 illustrates the network utility behavior for different frameworks and also a traditional LTE network (referred to as TN) using optimal GP values (i.e., $GP_{opt} = 4$ when $\alpha = 1.4$ and $GP_{opt} = 5$ when $\alpha = 3.0$). In all the scenarios, HVN has the best utility behavior. For mid-range values of w_c (e.g., when $w_c = 0.4 - 0.8$ in scenario 2 of Table VII), the HVN clearly has the best utility performance. For lower or higher w_c values, the LVN and the CVN approaches ultimately match the HVN in utility performance at either end of the w_c range, respectively, but never outperform it. Acknowledging both facts that HVN offers lower cost than the LVN at lower w_c values and higher QoS than the CVN at higher w_c values, it stands up unambiguously as the best network design choice. The value of w_c is a subjective design choice that depends on given MVON's/SP's investment constraints and intended services.

E. Optimal CVN Network Coefficient p_c^{opt} vs. Cost Weight w_c and Optimal CPC Radius \bar{d}_{cpc}^{opt}

To observe the dependence of the deployment ratio of CVN and LVN on the cost weight w_c , Fig. 12 shows the optimal

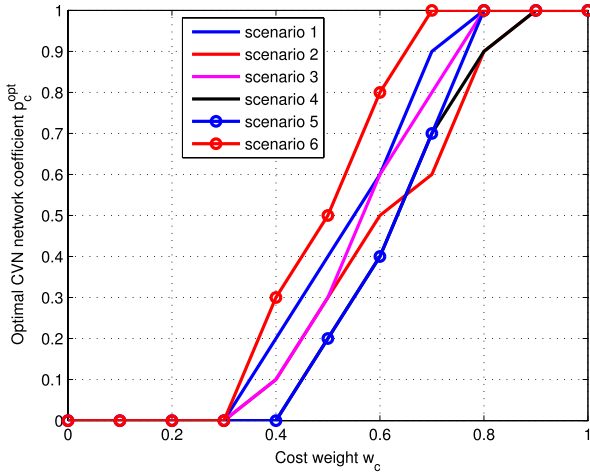


Fig. 12. Optimal CVN network coefficient p_c vs. cost weight w_c in different scenarios (cf. Table VII).

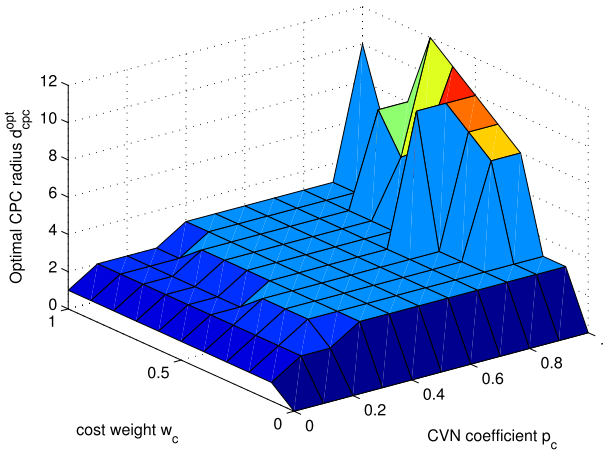


Fig. 13. Optimal CPC radius \bar{d}_{cpc}^{opt} vs. CVN network coefficient p_c vs. cost weight w_c in scenario I (cf. Table VII).

CVN network weight coefficient p_c^{opt} within a HVN for different w_c values. It is observed that for lower cost weights (i.e., $0 \leq w_c \leq 0.3$ (0.4 for scenario-5)), when very high QoS is required, the optimal CVN coefficient is $p_c=0$, which means that the whole network should be a LVN. If the offered service has lower QoS demand (e.g., file transfer, non real time applications, etc.), the SP should opt for building its network from the virtual resources of a data center (CPC). In contrast, if the offered service has strict QoS demand (e.g., voice, live video, etc.), the SP should integrate a larger share of special purpose hardware (LVN) that guarantees much faster PHY and MAC layer processing and also much lower transmission delays.

To have an overall idea of the dependence of the CVN network coefficient p_c on the optimal CPC radius \bar{d}_{cpc}^{opt} , and cost weight, w_c , we plot in Fig. 13, its variation with \bar{d}_{cpc}^{opt} and w_c . It is to be noted that for a low CVN coefficient (i.e., $p_c = 0.1$), the optimal CPC radius \bar{d}_{cpc}^{opt} is independent of the cost weight w_c , which is intuitive because if most of the wireless coverage is provided by distributed SBSs, a smaller wireless data center (i.e., a lower d_{cpc}) is sufficient

for CVN coverage of rest of the area. But it is interesting to note that as coverage by a CVN is increased (i.e., when $0.1 \leq p_c \leq 0.7$), a CPC with radius 2 to 3 km is optimal design choice. This indicates that even if most of the wireless coverage is done through CVNs, the size of the CPCs should remain smaller. This is because of the fact that as d_{cpc} increases, the length of the fiber-optic cables that connect the RRHs to the CPCs, also increases which in turn, increases the RTTD of the signals transmitted from the CPCs to the RRHs and vice-versa. Such an increase in RTTD degrades the achievable throughput, hence the lower QoS. For this reason, a lower d_{cpc} is preferred by the utility model (cf. equation (44)).

VIII. CONCLUSION

Wireless network virtualization is considered as an important component of future 5G networks for their ability to enable efficient resource sharing and to promote network innovation by providing greater flexibility in network design. Wireless networks vary widely in terms of the services they provide and also the radio access technologies they use. For this reason, implementing a generalized virtualization architecture that enables deployment of different kinds of virtual wireless networks is a challenging issue. In this paper, we propose three different models for wireless access network virtualization that differ in terms of their underlying physical infrastructures. The models have different set-up and operational costs; their performance also varies in terms of achievable network QoS. In the presence of multiple possible frameworks, the selection of an appropriate model for a certain scenario is a critical multidimensional challenge. In order to compare the proposed virtualization frameworks, we have built a composite multi-criteria utility model that considers both the economic and technical aspects (from PHY-MAC layer efficiencies) of the frameworks. It has been found that MAC layer parameters such as the guard period (GP) in an OFDM frame structure can be optimized from a network's cost-QoS perspective. The composite utility model presented in this article provides guidance to network designers on choosing a network model that fulfil the operator's investment target and service requirement constraints. It is observed that the CVN/RVN model has a cost advantage while the LVN provides a better QoS guarantee. For a network design, neither *only network cost* (i.e., $w_c = 1$) nor *only achievable QoS* (i.e., $w_c = 0$) can be of concern. There must be a compromise between the two. From the analytical results presented in this paper, it can be concluded that, the HVN can in fact, attain a balance between network cost & QoS according to a VNO's/SP's investment constraint and service provisioning goal. In order to make the analysis tractable, a rather simplified model has been assumed for network performance analysis. This model does not consider advanced PHY-MAC technologies such as coordinated multi point (CoMP), joint resource scheduling and processing among neighbouring BSs, interference management for a centralized control plane architecture, etc. In our future work, we shall include these features in the analysis of the frameworks along with the hand-off and interference management phenomena in multi-RAT HetNets.

REFERENCES

- [1] X. Zhou and L. Chen, "Demand shaping in cellular networks," in *Proc. Annu. Allerton Conf. Commun., Control Comput.*, Sep./Oct. 2014, pp. 621–628.
- [2] K. Pentikousis, Y. Wang, and W. Hu, "Mobileflow: Toward software-defined mobile networks," *IEEE Commun. Mag.*, vol. 51, no. 7, pp. 44–53, Jul. 2013.
- [3] S. Perez, J. M. Cabero, and E. Miguel, "Virtualization of the wireless medium: A simulation-based study," in *Proc. IEEE VTC*, Apr. 2009, pp. 1–5.
- [4] Y. Zaki, L. Zhao, C. Goerg, and A. Timm-Giel, "A novel LTE wireless virtualization framework," in *Proc. MONAMI*, Sep. 2010, pp. 245–257.
- [5] S. Singhal, G. Hadjichristofi, I. Seskar, and D. Raychaudhuri, "Evaluation of UML based wireless network virtualization," in *Proc. Next Generat. Internet Netw.*, Kraków, Poland, Apr. 2008, pp. 223–230.
- [6] G. Bhanage, I. Seskar, R. Mahindra, and D. Raychaudhuri, "Virtual basestation: Architecture for an open shared WiMAX framework," in *Proc. VISA*, Sep. 2010, pp. 1–8.
- [7] G. Bhanage, D. Vete, I. Seskar, and D. Raychaudhuri, "SplitAP: Leveraging wireless network virtualization for flexible sharing of WLANs," in *Proc. IEEE GLOBECOM*, Dec. 2010, pp. 1–6.
- [8] R. Kokku, R. Mahindra, H. Zhang, and S. Rangarajan, "NVS: A substrate for virtualizing wireless resources in cellular networks," *IEEE/ACM Trans. Netw.*, vol. 20, no. 5, pp. 1333–1346, Oct. 2012.
- [9] K.-K. Yap *et al.*, "Blueprint for introducing innovation into wireless mobile networks," in *Proc. 2nd ACM SIGCOMM Workshop Virtualized Infrastruct. Syst. Archit. (VISA)*, Sep. 2010, pp. 25–32.
- [10] Z. Zhu, Q. Wang, Y. Lin, P. Gupta, S. Kalyanaraman, and H. Franke, "Virtual base station pool: Towards a wireless network cloud for radio access networks," in *Proc. 8th ACM Int. Conf. Comput. Frontiers*, May 2010, pp. 1–10.
- [11] M. Chiosi *et al.*, "Network function virtualization: An introduction, benefits, enablers, challenges & call for action," in *Proc. SDN OpenFlow World Congr.*, Oct. 2012.
- [12] *iJOIN Project, Revised Definition of Requirements and Preliminary Definition of the iJOIN Architecture*, document INFSO-ICT-317941 iJOIN, D5.1, version 1.0.
- [13] T. Lin, J. M. Kang, H. Bannazadeh, and A. Leon-Garcia, "Enabling SDN applications on software-defined infrastructure," in *Proc. IEEE NOMS*, May 2014, pp. 1–7.
- [14] C. J. Bernardos *et al.*, "An architecture for software defined wireless networking," *IEEE Wireless Commun.*, vol. 21, no. 3, pp. 52–61, Jun. 2014.
- [15] L. E. Li, Z. M. Mao, and J. Rexford, "Toward software-defined cellular networks," in *Proc. IEEE EWSN*, Oct. 2012, pp. 7–12.
- [16] G. Karagiannis *et al.*, "Mobile cloud networking: Virtualisation of cellular networks," in *Proc. Int. Conf. Telecommun.*, 2014.
- [17] "C-RAN: The road towards green RAN," China Mobile Res. Inst., White Paper, Version 2.5, Oct. 2011.
- [18] P. Rost *et al.*, "Cloud technologies for flexible 5G radio access networks," *IEEE Commun. Mag.*, vol. 52, no. 5, pp. 68–76, May 2014.
- [19] K. Sundaresan, M. Y. Arslan, S. Singh, S. Rangarajan, and S. V. Krishnamurthy, "FluidNet: A flexible cloud-based radio access network for small cells," in *Proc. MobiCom*, Sep. 2013, pp. 99–110.
- [20] L. Zhou, X. Wang, W. Tu, G. Muntean, and B. Geller, "Distributed scheduling scheme for video streaming over multi-channel multi-radio multi-hop wireless networks," *IEEE J. Sel. Area Commun.*, vol. 28, no. 3, pp. 409–419, Apr. 2010.
- [21] Y. S. Soh, T. Q. S. Quek, M. Kountouris, and H. Shin, "Energy efficient heterogeneous cellular networks," *IEEE J. Sel. Areas Commun.*, vol. 31, no. 5, pp. 840–850, May 2013.
- [22] K. Johansson, A. Furuskar, P. Karlsson, and J. Zander, "Relation between base station characteristics and cost structure in cellular systems," in *Proc. IEEE PIMRC*, Sep. 2004, pp. 2627–2631.
- [23] L. Kruschwitz and A. Loeffler, *Discounted Cash Flow: A Theory of the Valuation of Firms*. West Sussex, U.K.: Wiley, 2005.
- [24] F. Loizillon *et al.*, *Final Results on Seamless Mobile IP Service Provision Economics*, document IST-2000-25172 TONIC Deliverable number 11, Oct. 2002.
- [25] H. Lehpamer, *Transmission Systems Design Handbook for Wireless Networks*. London, U.K.: Artech House, 2002.
- [26] D. E. Borth, "TDMA communications system with adaptive equalization," U.S. Patent 4852090 A, Jun. 25, 1989. [Online]. Available: <https://www.google.com/patents/US4852090>
- [27] *Evolved Universal Terrestrial Radio Access (E-UTRA); Physical Channels and Modulation (Release 9)*, document 3GPP TS 36.211, v9.1.0(2010-03).
- [28] N. McKeown *et al.*, "OpenFlow: Enabling innovation in campus networks," *ACM SIGCOMM Comput. Commun. Rev.*, vol. 38, no. 2, pp. 69–74, Apr. 2008.
- [29] P. Xing, L. Yang, C. Q. Li, P. Demestichas, and A. Georgakopoulos, "Multi-RAT network architecture," Wireless World Res. Forum, White Paper, Version 2.0, Nov. 2013.
- [30] R. Sherwood *et al.*, "FlowVisor: A network virtualization layer," Tech. Rep. OPENFLOW-TR-2009-1, Oct. 2009.
- [31] J. McCauley. *Pox: A Python-Based OpenFlow Controller*. [Online]. Available: <http://www.noxrepo.org/pox/about-pox/>
- [32] N. Gude *et al.*, "NOX: Towards an operating system for networks," *ACM SIGCOMM Comput. Commun. Rev.*, vol. 38, no. 3, pp. 105–110, Jul. 2008.
- [33] Ryu. [Online]. Available: <http://osrg.github.io/ryu/>
- [34] *Floodlight, An Open SDN Controller*. [Online]. Available: <http://www.projectfloodlight.org/floodlight/>
- [35] J. Reich, C. Monsanto, N. Foster, J. Rexford, and D. Walker, "Modular SDN programming with pyretic," in *Proc. USENIX Mag.*, vol. 38, Oct. 2013, pp. 40–47.
- [36] *OpenStack*. [Online]. Available: <http://www.openstack.org>
- [37] M. M. Rahman, C. Despins, and S. Affes, "Service differentiation in software defined virtual heterogeneous wireless networks," in *Proc. IEEE ICUBW*, Oct. 2015, pp. 1–5.
- [38] C. D. Patel and A. J. Shah, "Cost model for planning, development and operation of a data center," Hewlett-Packard Develop. Company, L.P., Palo Alto, CA, USA, Tech. Rep., 2005. [Online]. Available: <http://www.hpl.hp.com/techreports/2005/HPL-2005-107R1.pdf>
- [39] *Mininet: An Instant Virtual Network on Your Laptop (or Other PC)*. [Online]. Available: <http://mininet.org/>
- [40] *OpenvSwitch*, accessed on Dec. 7, 2015. [Online]. Available: <http://openvswitch.org/>
- [41] M. M. Rahman, C. Despins, and S. Affes, "Analysis of CAPEX and OPEX benefits of wireless access virtualization," in *Proc. IEEE ICC*, Jun. 2013, pp. 436–440.
- [42] L. Nuaymi, *WiMAX: Technology for Broadband Wireless Access*. West Sussex, U.K.: Wiley, 2007.
- [43] Q.-T. Nguyen-Vuong, N. Agoulmine, E. H. Cherkaoui, and L. Toni, "Multicriteria optimization of access selection to improve the quality of experience in heterogeneous wireless access networks," *IEEE Trans. Veh. Technol.*, vol. 62, no. 4, pp. 1785–1800, May 2013.



M. Moshir Rahman received the bachelor's degree in electronics and communications engineering from the University of Dhaka, Bangladesh, in 2005, and the M.Sc. degree in telecommunications engineering from the University of Trento, Italy, in 2011. He is currently pursuing the Ph.D. degree with ETS, University of Quebec, Canada. From 2005 to 2008, he was a Telecommunications Engineer for different mobile network operators in Bangladesh. From 2010 to 2011, he was a Visiting Research Student with INRS-EMT, University Quebec. He was a Wireless Researcher (Intern) with Huawei Technologies Canada from 2015 to 2016. He is a Technical Marketing Engineer with the Center of Excellence in Next Generation Networks, Ottawa, Canada. His research interests lie in the fields of wireless communications, network virtualization, software defined networking, and cloud computing technologies.



Charles Despins received the bachelor's degree in electrical engineering from McGill University, Montreal, QC, Canada, in 1984, and the master's and Ph.D. degrees from Carleton University, Ottawa, ON, Canada, in 1987 and 1991, respectively. He was with CAE Electronics as a member of the Technical Staff from 1984 to 1985, the Department of Electrical and Computer Engineering, École Polytechnique de Montréal, Canada, as a Lecturer and a Research Engineer from 1991 to 1992, and a Faculty Member with the Institut National de la Recherche Scientifique, Université du Québec, Montreal, from 1992 to 1996. From 1996 to 1998, he was with Microcell Telecommunications Inc., a Canadian GSM operator, and was responsible for industry standard and operator working groups, as well as for technology trials and technical support for joint venture deployments in China and India. From 1998 to 2003, he was the Vice President and Chief Technology Officer of Bell Nordiq Group Inc., a wireless and wireline network operator in northern and rural areas of Canada. From 2003 to 2016, he was the President and CEO of Prompt Inc., a university-industry research consortium in the field of information and communications technologies. He is currently a Faculty Member with the École de Technologie Supérieure (Université du Québec), with research interests in wireless communications. He is also a Guest Lecturer in the M.B.A. program with McGill University, Montreal. He received the IEEE Vehicular Technology Society Best Paper of the Year prize in 1993, and the Outstanding Engineer Award in 2006 from the IEEE Canada. He is a member of the Order of Engineers of Québec and was also a fellow (2005) of the Engineering Institute of Canada.



Sofiene Affes (S'94-M'95-SM'05) received the Diplôme d'Ingénieur degree in telecommunications and the Ph.D. degree (Hons.) in signal processing from the École Nationale Supérieure des Télécommunications, Paris, France, in 1992 and 1995, respectively. He was a Research Associate with INRS, Montreal, QC, Canada, until 1997, an Assistant Professor until 2000, and an Associate Professor until 2009. He is currently a Full Professor and Director of PERSWADE, a unique \$4M research training program on wireless in Canada involving 27 faculty members from eight universities and ten industrial partners. From 2003 to 2013, he was a Canada Research Chair in wireless communications. He served as a General Co-Chair of the IEEE VTC'2006-Fall and the IEEE ICUWB'2015, respectively, both held in Montreal. He is an Associate Editor of the IEEE TRANSACTIONS ON COMMUNICATIONS and the *Wiley Journal on Wireless Communications and Mobile Computing*. He was an Associate Editor of the IEEE TRANSACTIONS ON WIRELESS COMMUNICATIONS from 2007 to 2013, and the IEEE TRANSACTIONS ON SIGNAL PROCESSING from 2010 to 2014. He was a recipient of a Discovery Accelerator Supplement Award twice from NSERC from 2008 to 2011 and from 2013 to 2016. In 2008 and 2015, he received the IEEE VTC Chair Recognition Award from the IEEE VTS and the IEEE ICUWB Chair Recognition Certificate from the IEEE MTT-S for exemplary contributions to the success of the IEEE VTC and the IEEE ICUWB, respectively.